# C h a p t e r 3

## Ring-Expansion Metathesis Polymerization:

## Catalyst Dependent Polymerization Profiles

Portions of this chapter have been published: Xia, Y.; Boydston, A. J.; Yao, Y.; Kornfield, J. A.; Gorodetskaya, I. A.; Spiess, H. W.; Grubbs, R. H. *J. Am. Chem. Soc.* **2009**, 131, 2670-2677.

**Abstract**

Ring-expansion metathesis polymerization (REMP) mediated by recently developed cyclic Ru catalysts has been studied in detail with a focus on the polymer products obtained under varied reaction conditions and catalyst architectures. Depending upon the nature of the catalyst structure, two distinct molecular weight evolutions were observed. Polymerization conducted with catalysts bearing 6-carbon tethers displayed rapid polymer molecular weight growth which reached a maximum value at ca 70% monomer conversion, resembling chain-growth polymerization mechanism. In contrast, 5-carbon tethered catalysts lead to molecular weight growth that resembled a step-growth mechanism with a steep increase occurring only after 95% monomer conversion. The underlying reason for these mechanistic differences appeared to be ready release of 5-carbon tethered catalysts from growing polymer rings, which competed significantly with propagation. Owing to reversible chain transfer and the lack of end groups in REMP, the final molecular weights of cyclic polymers was controlled by thermodynamic equilibria. Large ring sizes in the range of 60 – 120 kDa were observed at equilibrium for polycyclooctene and polycyclododecatriene, which were found to be independent of catalyst structure and initial monomer/catalyst ratio. While 6-carbon tethered catalysts slowly incorporated into the formed cyclic polymer, the incorporation of 5-carbon tethered catalysts was minimal, as revealed by ICP-MS. Further polymer analysis was conducted using melt-state magic-angle spinning $^{13}C$ NMR spectroscopy and matrix-assisted laser desorption ionization mass spectrometry of both linear and cyclic polymers, which revealed little or no chain ends for the latter topology.

## Introduction

Cyclic polymers have been a fascinating macromolecular architecture for synthetic chemists, as well as materials scientists and physicists, since the discovery of circular DNA.[1-2] Constraining a macromolecule into a cyclic topology can result in unique properties in comparison with linear analogues such as lower viscosities, smaller hydrodynamic radii, and increased functional group density.[1-3] Furthermore, cyclic polymers may challenge and expand fundamental knowledge regarding polymer properties as they relate to the presence and absence of chain ends. These characteristics make cyclic polymers interesting targets for studying fundamental aspects of property-topology relationships as well as new resources in materials science. Despite considerable recent development in the area of cyclic polymers, the full potential of these materials is yet to be realized. Further advancement requires the ability to efficiently prepare large-scale quantities of cyclic polymers spanning a diverse range of functionality and controlled molecular weights.

From a synthetic standpoint, cyclic polymers present a unique challenge in polymer chemistry. Successful production of large macrocycles has traditionally been accomplished by macrocyclization of appropriately end-functionalized telechelic polymers.[4] Although this approach is compatible with both symmetric[5-12] and unsymmetric[13-16] telechelic polymers, as well as triblock copolymers,[17-18] inherent limitations still persist. Specifically, macrocyclization is generally limited to low polymers (i.e., <10 kDa), and requires high-dilution conditions to suppress intermolecular reaction of end groups. A recent breakthrough in obtaining high molecular weight cyclic polymers utilized macrocyclization of triblock copolymers under high dilution

conditions.[17-18] Using an ABC triblock system in which the A and C blocks comprised complementary coupling partners, this approach provided a mixture of linear and cyclic polymers of up to 96 kDa. The cyclization efficiency for these high molecular weight triblocks was much greater than that typically observed for traditional macrocyclization of telechelic polymers due to the greatly increased effective concentration of functional groups in the A and C blocks of the former. Other cyclic polymer syntheses include those relying on back-biting events during ring-chain equilibria[19-20] or linear living polymerizations.[21] The scope of such methods, however, remains narrow in comparison with the macrocyclization methods previously mentioned.

Complementary to the "grow-then-cyclize" approach of macrocyclization, an alternative strategy, which may be viewed as a "grow-while-cyclic" method, involves ring-expansion of cyclic monomers.[22-30] For example, Pd-mediated polymerization of methylidenecyclopropanes was demonstrated by Osakada, and achieved metallacycles of 5.3 kDa.[25] The prospect of high fidelity ring-expansion methodology offers the potential for formation of pure cyclic polymers free of linear contaminants and to improve the efficiency with which such materials are produced.

The series of cyclic Ru-alkylidene catalysts developed in the Grubbs group (Figure 1), as discussed in Chapter 1, resembled olefin metathesis catalyst **1**, and were able to mediate ring-expansion metathesis polymerization (REMP) of cyclic olefins to produce cyclic polymers.[22,29-30] Overall, REMP has several distinct advantages, such as: 1) the potential to produce large quantities of cyclic polymers from readily available cyclic monomers; 2) tolerance for high concentration, including bulk polymerizations; 3) the

ability to produce homopolymers without linkage groups, including pure hydrocarbon macrocycles; and 4) access to a broad range of molecular weights, extending up to $10^6$ Da.

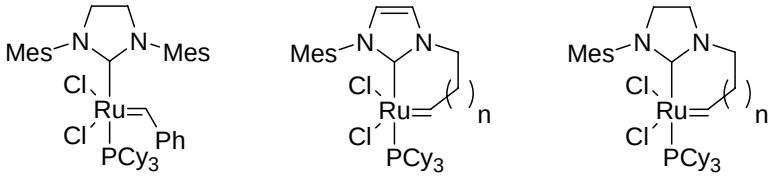


**1** **UC-5**, n = 3 **UC-6**, n = 4 **SC-5**, n = 3 **SC-6**, n = 4

**Figure 1.** Olefin metathesis catalyst **1** and cyclic REMP catalysts.

Capitalizing on the attributes mentioned above requires deeper insights into the mechanism of REMP and an ability to control polymer molecular weights and product distribution by guiding metathesis events within the catalytic cycle. The activities of Ru-based metathesis catalysts can be finely tuned via structural modulation,[31-34] and we envisioned that the specific structural differences in cyclic catalysts (Figure 1) may offer a means to guide the relative rates of different metathesis events involved in REMP, as indicated by our catalyst-focused study in chapter 1. The most apparent mechanistic steps involved in REMP include catalyst initiation, propagation, catalyst release, and intramolecular chain transfer (Figure 2). The rate of initiation (given rate constant $k_i$) determines the number of catalyst molecules which enter the catalytic cycle, and may also influence the total number of polymer rings which are ultimately formed. Chain propagation, represented by the rate constant $k_p$, is expected to be independent of catalyst tether length and dependent on NHC electronics (i.e., saturated versus unsaturated backbones). Due to the possibility of catalyst release (with rate constant $k_r$) and re-incorporation ($k_{-r}$) during REMP, the value of $k_p$ cannot be directly determined based on the overall polymerization rates alone. Importantly, it is the relative rates of each of these events that will dictate the kinetically controlled product distribution.

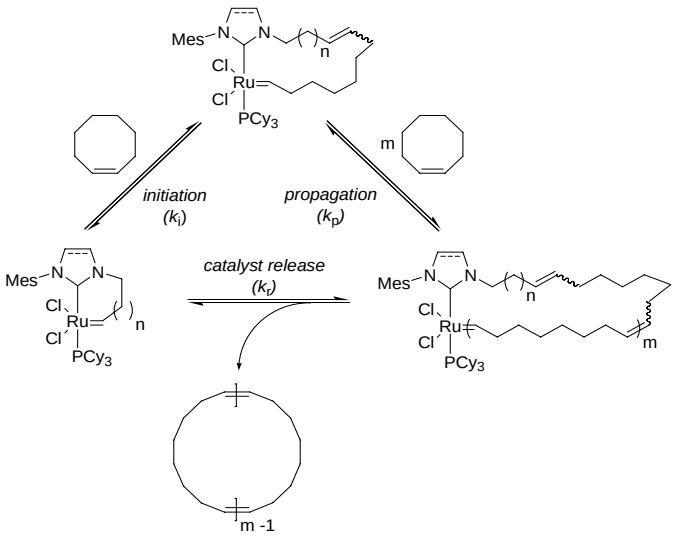


**Figure 2.** Key mechanistic steps involved in REMP.

In a simplified case, the average degree of polymerization (DP) would be given by $DP = k_p[\text{monomer}]/k_r$ (1)

In such cases, chain growth mechanism would be expected to dominate when $k_p[\text{monomer}] >> k_r$. In contrast, for $k_p[\text{monomer}] \sim k_r$, step growth molecular weight increase would be expected. Both intra- and intermolecular chain transfer events, however, must also be considered during REMP, and therefore Eq (1) cannot be applied to polymerization involving such events. As depicted in figure 3, the ability of an incorporated (i.e., propagating) catalyst species to interact with olefins within the polymer backbone, in a manner that does not result in release of the original catalyst, may be regarded as polymer "pinching" and is assigned the rate constant $k_t$. Polymer pinching would yield two separate macrocycles of reduced, and not necessarily equal, molecular weight. Dependent upon the number and placement of Ru complexes in the initial ring, at least one of the ensuing macrocycles would contain an active catalyst species and could either undergo chain growth or further pinching. Intermolecular chain transfer ($k_{-t}$), which may be viewed as the reverse of polymer pinching or polymer "fusion", would result in

considerable molecular weight growth since two large ring systems are being combined. Notably, the reversibility of olefin metathesis provides a potential avenue toward thermodynamic molecular weight control over "endless" polymers via polymer pinching and macrocyclic combination.

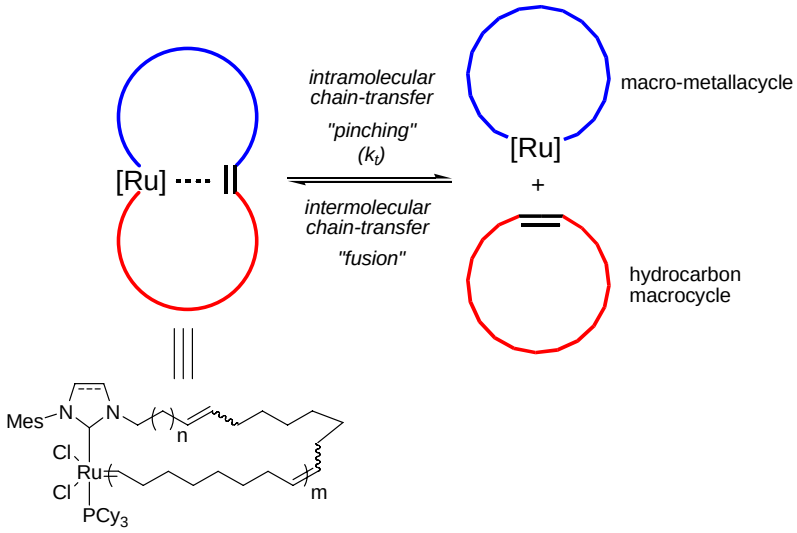


**Figure 3.** Depiction of reversible polymer "pinching" via intramolecular chain transfer and "fusion" via intermolecular chain transfer.

We envisioned that catalyst structure and reaction conditions could be tuned to control the relative values of $k_i$, $k_p$, $k_r$ and $k_t$ and ultimately facilitate access to different kinetically controlled polymer product distributions. The origins of the faster conversions of monomer to polymer, however, may be due to faster initiation, slower catalyst release, faster propagation, or some combination thereof. Catalysts bearing 5-carbon tethers (i.e., **UC-5** and **SC-5**) showed no incorporation into the polymer during polymerizations, suggesting an equilibrium had been established that strongly favored a non-incorporated resting state of the cyclic catalysts. This observation corresponds to catalyst behavior involving initiation, incorporation of monomer units, and catalyst release all prior to complete consumption of monomer; therefore the catalyst does not reside in the formed

polymer. This would be expected to provide multiple polymer macrocycles from each catalyst molecule, and potentially display molecular weight growth reminiscent of step-growth mechanisms.

Herein, predictions regarding polymer structure based on our previous catalyst-focused investigations are tested by examining polymer products during and after polymerization. Collectively, the results demonstrate how different catalyst architectures may be used to control the kinetic profiles of REMP. We describe herein comparative studies of cyclic polymers obtained via REMP of cyclooctene (COE), cyclododecatriene (CDT), and cyclooctene macrocycles (e.g., cyclic cyclooctene trimer), with particular focus on catalyst initiation rates, polymer molecular weight evolution during and after polymerization, quantification of Ru in the cyclic polymer products, and application of melt-state $^{13}C$ NMR spectroscopy for the characterization of cyclic polymers.

**Results and Discussion**

**Initiation.** Catalyst initiation is an important parameter, governing the amount of catalyst that enters the REMP cycle and thus the number of growing chains in solution. In the case of REMP, catalyst release during polymerization may also influence the overall rate of conversion because it competes with propagation, thus it is important to examine the catalyst initiation rates independently. Furthermore, resting state and propagating REMP catalyst species are different in nature, and it has been observed that initiation rates of Ru complexes are not always directly proportional to their olefin metathesis activities.[33]

To investigate REMP catalyst initiation rates, we measured the initiation kinetics by monitoring the stoichiometric metathesis reaction of **1**, **UC-5**, **SC-5**, **UC-6** and **SC-6** each with butyl vinyl ether (BVE).[33-34] Each catalyst was treated with an excess of BVE

(30 equiv relative to [Ru]) in $C_6D_6$ at 60 °C and the reaction progress was monitored by $^1$H NMR spectroscopy. Regioselective conversion of the alkylidene complexes (**A**) to the corresponding Fischer carbenes (**B**) was observed for each catalyst and key data are summarized in Table 1. All reactions showed clean first-order kinetics over the time investigated.

**Table 1.** Initiation kinetics via $^1$H NMR spectroscopy[a]

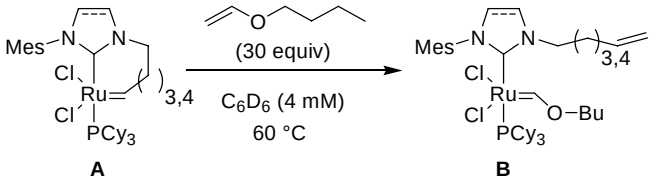


**A** **B**

| catalyst | $k_{obsd}$ ($s^{-1}$) | $k_{rel}$[b] |
|---|---|---|
| **1** | $8.2 \times 10^{-3}$ | 1 |
| **SC-5** | $1.1 \times 10^{-2}$ | 1.3 |
| **UC-5** | $2.4 \times 10^{-3}$ | 0.29 |
| **SC-6** | $4.2 \times 10^{-4}$ | 0.051 |
| **UC-6** | $5.0 \times 10^{-5}$ | 0.0061 |

[a]Conditions: $[Ru]_0 = 0.004$ M in $C_6D_6$ at 60 °C under $N_2$ (sealed tube); $[BVE/Ru]_0 = 30:1$.
[b]$k_{rel}$ is the relative rate constant with respect to catalyst **1**.

The initiation rates showed a strong dependence on the catalyst structure (Table 1). Both **UC-5** and **SC-5** displayed dramatically increased initiation rates in comparison with their 6-carbon tether counterparts, **UC-6** and **SC-6**. Specifically, shortening the tether length by one carbon atom increased the initiation rate by 25 and 48 times for catalysts with saturated and unsaturated NHCs, respectively. In addition, saturation of the NHC backbone also improved initiation as reported for other Ru-NHC complexes.[33] Notably, **SC-5** was found to initiate slightly faster than complex **1** under identical conditions.

**Rate of Polymerization.** To compare the rate of polymerization for **UC-4** – **UC-7** in REMP, we examined their relative efficiencies in the polymerization of cyclooctene (COE) to poly(cyclooctene) (PCOE). As can be seen from the data presented in Figure 4, the relative efficiencies of the catalysts showed a strong dependence on the length of the chelating tether. In general, increased tether length was accompanied by an increase in catalytic activity. For example, comparison of the unsaturated catalysts revealed the time required to reach >95% conversion was nearly 24 h for **UC-4** (green line), approximately 8 h for **UC-5** (purple line) and **UC-6** (blue line), and less than1 h for **UC-7** (red line).

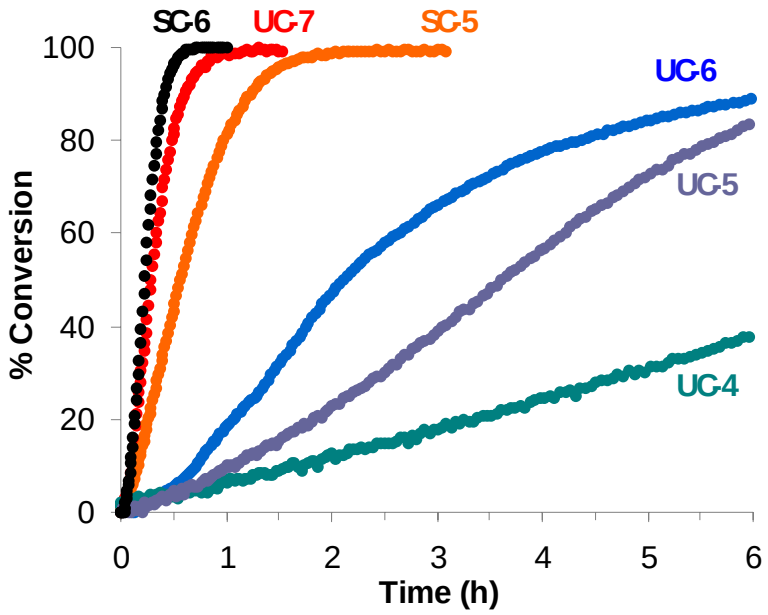


**Figure 4**. REMP of COE using catalysts **UC-4** (green), **UC-5** (purple), **SC-5** (orange), **UC-6** (blue), **SC6** (black), and **UC-7** (red). Conditions: $CD_2Cl_2$, 40 °C, $[M/C]_0$ = 1000:1, $[M]_0$ = 0.5 M. Conversion determined by $^1H$ NMR spectroscopy.

Saturation of the NHC backbone was found to dramatically increase catalyst activity. As expected, **SC-5** and **SC-6** each displayed faster polymerization rates than their unsaturated analogues **UC-5** and **UC-6**, respectively (Figure 4). Surprisingly, the polymerization rate acceleration resulting from NHC saturation appeared to be greater

than for homologation of the tether length. Specifically, **SC-6** was found to achieve >95% conversion in shorter reaction times than did **UC-7**. Similarly, **SC-5** was found to be a more active polymerization catalyst than **UC-6**. Overall, the data revealed that judicious combinations of shorter tether lengths (i.e., 5- or 6-carbon tethers) and NHC backbone saturation (e.g., **SC-5** and **SC-6**) provide a desirable balance of catalyst stabilities and activities.

Interestingly, the effects of ligand structure on relative rates of polymerization do not correspond directly with the observed initiation rates. In particular, the observed rates of polymerization were in the order of **SC-6** > **SC-5** > **UC-6** > **UC-5**, however, the significantly faster initiation of the C-5 catalysts is surprising. After the insertion of the first monomer, further insertions are not expected to depend on a single carbon difference in the size of the ring. Therefore, slower polymerization for C-5 vs. C-6 analogues is not attributed to a difference in the rate constant for monomer addition. Instead, the decreased polymerization rate of C-5 catalysts—in spite of their faster initiation—supports our previous hypothesis that the catalyst release is strongly favored over polymer propagation for these systems.

Catalyst stability takes on particular importance in REMP as decomposition of the catalyst before, during, or after polymerization could potentially lead to linear polymers, instead of the envisioned macrocycles. In addition, relative stabilities are important factors in the general development of new metathesis catalysts. Furthermore, it has been observed in some systems that catalyst stability and activity are inversely related.[35] To explore the stabilities of REMP catalysts **UC-4** – **UC-7** during polymerization reactions, we plotted the ln([COE]) versus time for REMP of COE (Figure 5). The logarithmic plots

were found to be linear ($R^2$ values ranged from 0.969 to 0.997) between 20% and 80% conversion of COE to PCOE, indicating that catalyst decomposition was negligible in all cases during the time of the polymerization reactions. Closer examination of the plots revealed that the only discernable deviations from linearity (i.e., pseudo-first-order rate kinetics) involved apparent increases in the rate of monomer consumption. This observation can be rationalized by a relatively slow initiation period which would manifest in a gradual increase in the number of propagating polymer chains, and concomitant increase in the rate of conversion.

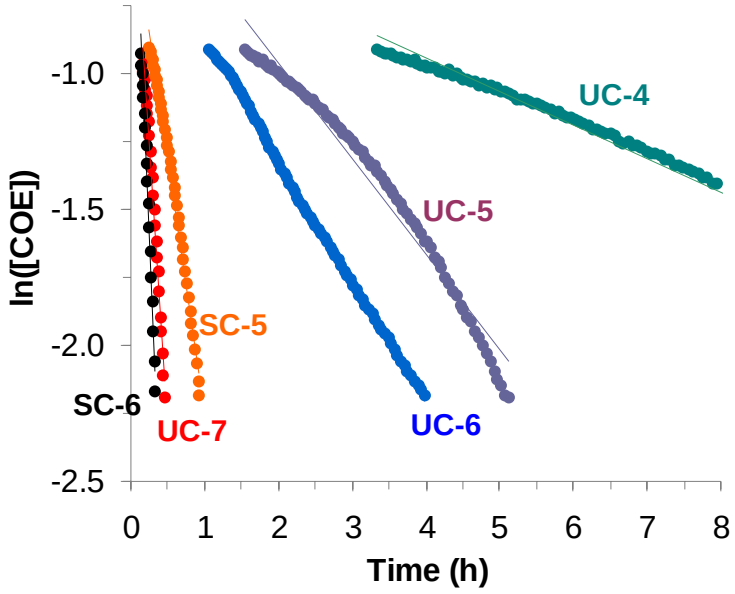


**Figure 5**. Log plots for REMP of COE using catalysts **UC-4** (green), **UC-5** (purple), **SC-5** (orange), **UC-6** (blue), **SC-6** (black), and **UC-7** (red). Linear least-squares fitting gave $R^2$ values of: **UC-4**, 0.997; **UC-5**, 0.969; **SC-5**, 0.991; **UC-6**, 0.998; **SC-6**, 0.990; and **UC-7**, 0.991. Conditions: $CD_2Cl_2$, 40 °C, $[M/C]_0$ = 1000:1, $[M]_0$ = 0.5 M. Conversion determined by $^1$H NMR spectroscopy.

**Molecular Weight Growth and Decline.** The molecular weight evolution during polymerization, and equilibration of the cyclic polymers after complete monomer consumption, can shed light on the relative values of $k_p$, $k_r$ and $k_t$. For a specific monomer,

different catalysts may be useful for guiding the molecular weight evolution of the cyclic polymers.

We monitored the molecular weight of PCOE during the REMP of COE using cyclic catalysts **UC-6**, **SC-6**, **UC-5**, and **SC-5**. Tether length was found to strongly affect the molecular weight versus conversion profiles (Figure 6), and in all cases the polydispersity indices (PDIs) ranged from 1.3 to 1.8. Catalysts **UC-6** and **SC-6** each delivered a large increase in molecular weight at the beginning of the polymerizations. Additionally, sharp increases in solution viscosities were observed within 1 h. PCOE obtained using **UC-6** displayed a peak molecular weight of 667 kDa when conversion reached 69%, followed by a drop in molecular weight such that at 100% conversion the molecular weight was found to be 393 kDa. Saturated catalyst **SC-6** displayed rapid molecular weight growth such that aliquots drawn prior to complete consumption of monomer provided polymers of sufficiently high molecular weight that they precluded molecular weight analysis via our GPC instrumentation. Thus, for comparison with the other catalyst systems, we use the first $M_w$ obtained of 1260 kDa at 100% conversion. The observed molecular weight evolution for **UC-6** and **SC-6** under these conditions corresponds to polymerization rates that are significantly greater than those of catalyst release or other intramolecular chain transfer reactions. As the concentration of monomer decreased and that of polymer increased, propagation slowed sufficiently such that polymer pinching ($k_t$) became competitive resulting in molecular weight decline, as discussed in the next section.

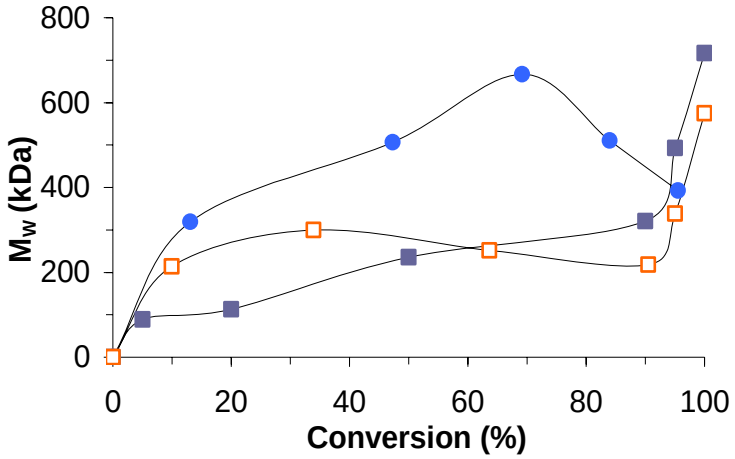


**Figure 6**. Weight-average molecular weight versus monomer conversion for the polymerization of COE using catalysts **UC-6** (●), **UC-5** (■), and **SC-5** (□). Conditions: $[COE]_0$ = 0.5 M in $CH_2Cl_2$ at 40 °C; $[COE/Ru]_0$ = 1000:1. (Polymer peaks were used to determine the molecular weight when separate oligomer peaks coexisted at low conversions using **UC-5** and **SC-5**.)

Interestingly, **UC-5** and **SC-5** were found to give strikingly different molecular weight growth profiles than their homologues **UC-6** and **SC-6** (Figure 6). In addition, the reaction mixtures did not show noticeable increase in viscosity until nearly complete monomer consumption, when rapid increase in viscosity was observed. In each case PCOE molecular weight increased sharply at low conversion (i.e., <10%) with noticeable amounts of oligomeric species detected by GPC analysis. Following this initial molecular weight increase, more gradual change in molecular weight, and concomitant decrease in the relative amounts of oligomer, were observed until approximately 90% conversion was achieved. At this point, sharp increases in molecular weight were observed reaching 575 and 717 kDa for **UC-5** and **SC-5**, respectively, at 100% conversion. The molecular weight evolution observed using the C-5 catalysts indicated a greater tendency for catalyst release during polymerization than their C-6 counterparts. Since the relative rates of monomer insertion and catalyst release regulate the kinetic molecular weight in REMP,

at high monomer concentrations propagation occurred faster than catalyst release, and thus polymeric species were observed even at low conversions. The rate of catalyst release, however, quickly became dominant as monomer concentration declined. The steep increase in molecular weight at high conversion suggested that macrocycles were combined via intermolecular chain-transfer events while remaining monomer continued to be incorporated. Notably, this data supports the notion that **UC-5** and **SC-5** each established an equilibrium during polymerization that strongly favored a non-incorporated resting state of the catalyst.

Once all of the monomer is consumed during REMP, the catalyst may continue to perform intra- and intermolecular chain transfer events on macrocyclic species, facilitating molecular weight equilibration. In the absence of end groups, the molecular weight of the final polymers at equilibrium should correspond to the ring size having the lowest thermodynamic energy under the experimental conditions. This differs from many linear polymerizations, including ring-opening metathesis polymerization (ROMP) in which the molecular weight is regulated by the amount of end groups present in the system, which are often from the initiator or chain transfer agent.

To investigate the molecular weight equilibration, we monitored the $M_w$ of the polymers after 100% monomer conversion. Each of the catalysts studied eventually arrived at PCOE $M_w$s ranging from 300–500 kDa (Figure 7). The broad range of final $M_w$s suggested that the equilibration had stopped, for example due to catalyst death. To continue the equilibration, we isolated the cyclic PCOE via precipitation into excess acetone. After redissolving and precipitating the polymer successively three times to remove residual catalyst, the polymer was redissolved in $CH_2Cl_2$ with an olefin

concentration of 0.5 M. Polymer solutions were then treated with REMP catalyst and heated at 40 °C. After 12 h, PCOE was iteratively precipitated three times into acetone and analyzed by GPC to determine the PCOE $M_w$. The process of polymer isolation, analysis, and subjection to polymerization conditions was repeated three times while maintaining an olefin concentration of 0.5 M in each round, until the change in $M_w$ was minimal. As shown in Figure 8, the PCOE $M_w$ declined rapidly during the first cycle, then more slowly in subsequent cycles, ultimately approaching a value of 60 kDa. The entire process was repeated using $PhCH_3$ in place of $CH_2Cl_2$, which lead to a final $M_w$ of 100 kDa.

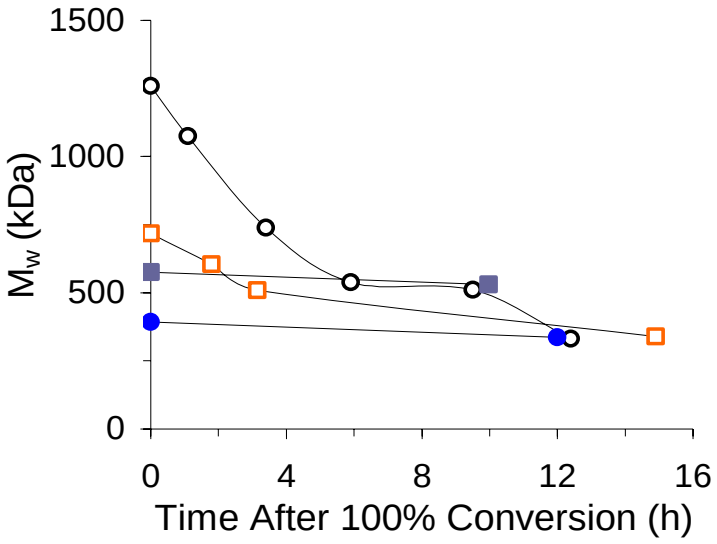


**Figure 7**. Equilibration of molecular weight of PCOE after 100% monomer conversion was obtained via REMP using catalysts **UC-6** (●), **SC-6** (○), **UC-5** (■), and **SC-5** (□). Conditions: $[COE]_0$ = 0.5 M in $CH_2Cl_2$ at 40 °C; $[COE/Ru]_0$ = 1000:1.

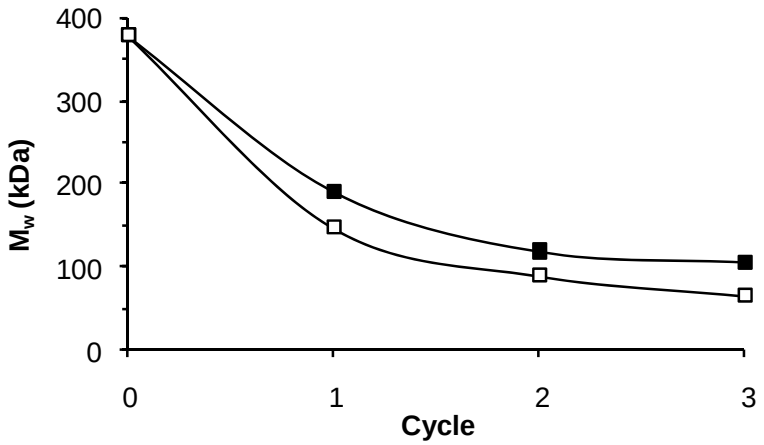


**Figure 8.** Molecular weight equilibrium of PCOE. Conditions: **SC-5** was repeatedly added at [olefin/Ru] = 500 to isolated PCOE, PCOE dissolved at 0.5 M (olefin concentration), 12 h, 40 °C in $PhCH_3$ (■) and in $CH_2Cl_2$ (□).

As mentioned previously, if the molecular weight evolution in REMP was approaching a thermodynamically stable state, catalyst loading should only impact the rate at which the equilibrium molecular weight is reached. Using similar conditions to those described above, but with varying initial monomer to catalyst ratios ($[M/Ru]_0$), we examined the molecular weight dependence on this variable. As shown in table 2, the $[M/Ru]_0$ did not linearly correlate with the final molecular weights obtained from the cyclic PCOE. Specifically, a $[M/Ru]_0$ of 1000:1 resulted in a PCOE molecular weight of 380 kDa, reflecting catalyst death prior to complete molecular weight equilibration (see above). Using $[M/Ru]_0$ of 300:1 or 100:1, however, resulted in a PCOE molecular weight of 150 and 100 kDa, respectively. Notably, the difference in molecular weights did not directly reflect the difference in $[M/Ru]_0$ used. Further reduction of the $[M/Ru]_0$ to 33:1 gave PCOE having a molecular weight of 70 kDa. Collectively, the results suggested that in the absence of considerable catalyst death, the final molecular weight more closely reflected thermodynamic equilibration, rather than $[M/Ru]_0$.

**Table 2.** Effect of **UC-6** catalyst loading on PCOE molecular weight[a]

| $[M/Ru]_0$ | $M_w$ (kDa) | PDI |
|---|---|---|
| 1000 | 380 | 1.6 |
| 300 | 150 | 1.5 |
| 100 | 100 | 1.8 |
| 33 | 70 | 1.6 |

[a]Conditions: $[COE]_0$ = 0.5 M in $CH_2Cl_2$ at 40 °C for 12 h.

We next explored the impact of monomer structure on the molecular weight evolution during REMP. Monomer characteristics, such as ring strain and olefin density, may strongly affect the relative rates of propagation and chain transfer. Therefore, we studied REMP of cyclododecatriene (CDT), which has less strain than COE and twice the olefin density, and would be expected to slow propagation but facilitate chain transfer. To test the hypothesis that REMP of CDT using C-5 catalysts would exhibit efficient catalyst release and as a result more step like molecular weight growth than REMP of COE, the molecular weight evolution was studied for CDT in $CH_2Cl_2$ (0.3 M) at 40 °C using $[CDT/\mathbf{SC\text{-}5}]_0$ = 500:1. The total monomer concentration was reduced in comparison with the experiments described above using COE ($[COE]_0$ = 0.5 M). The reduced monomer concentration is also expected to favor catalyst release over propagation.

Strikingly, although the monomer conversion reached completion in 4 h, only oligomeric species were observed suggesting that propagation is slower than catalyst release. Polymeric species were detectable by GPC only when conversion began to approach 90% (Figure 9), and relative amounts were significantly less than that of oligomeric species. Continued GPC analysis revealed that a polymer peak gradually

became dominant over lower molecular weight oligomers 8 h after full monomer conversion. After all the monomer was converted to oligomers, these small rings then coalesced into thermodynamically favored cyclic polymers through intermolecular chain transfer. Thus, the propagation of CDT at 0.3 M was sufficiently slower than chain transfer, leading to the observed step-growth type polymerization profile.

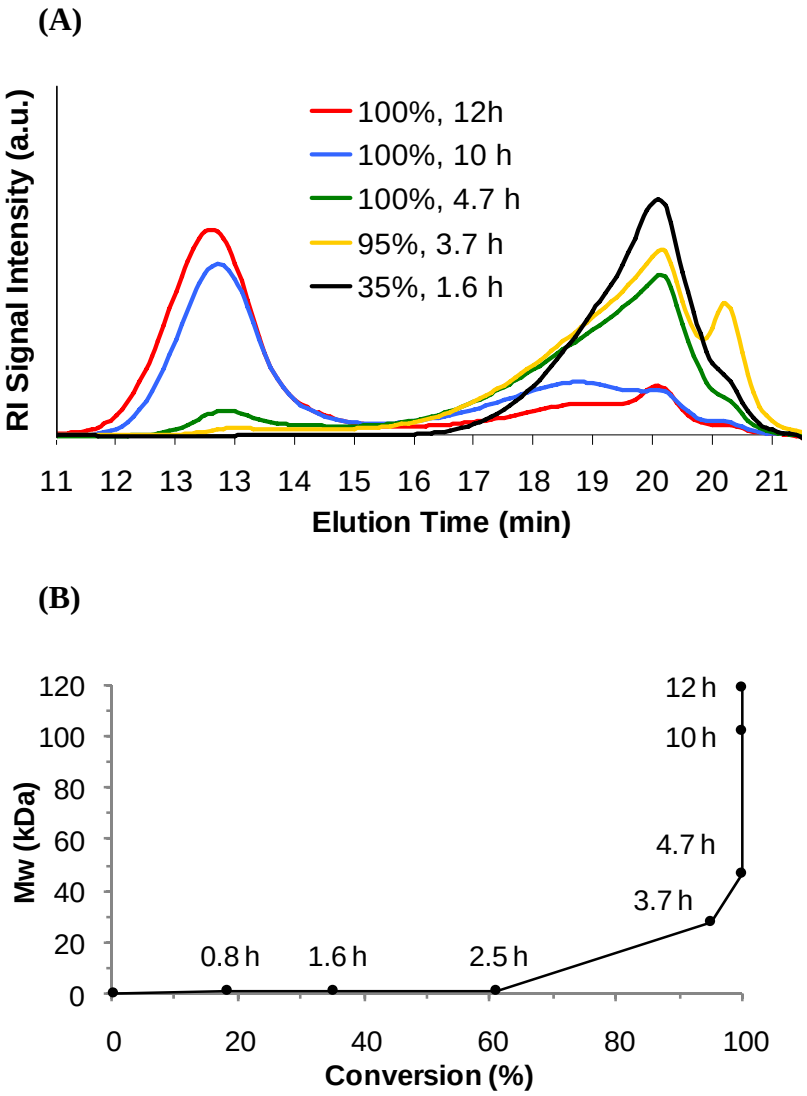


**Figure 9.** (A) GPC traces of REMP of CDT using **SC-5** at different conversions. (B) molecular weight vs. monomer conversion for REMP of CDT using **SC-5**. $[CDT]_0$ = 0.3 M in $CH_2Cl_2$, $[CDT/\mathbf{SC\text{-}5}]_0$ = 500:1, 40 °C. Aliquots were withdrawn at the indicated times and immediately treated with ethyl vinyl ether. Conversions were determined by $^1H$ NMR spectroscopy prior to GPC analysis. After the formation of polymeric species above 95% conversion, only the polymer peaks were selected to determine the molecular weight in figure 9B.

In contrast to REMP of CDT using **SC-5**, **SC-6** produced polymeric species even at low conversions, in addition to significant amounts of oligomer. This is in accord with the faster propagation previously observed from **SC-6** (cf. **SC-5**) in combination with sluggish catalyst release. Moreover, intramolecular chain transfer would be expected to

occur equally efficiently from either an incorporated **SC-5** or **SC-6** species. Therefore, the stunted molecular weight growth observed from **SC-5** can likely be ascribed specifically to increased catalyst release in comparison with **SC-6**, as opposed to ring "pinching" via intra-chain metathesis events.

The molecular weight growth observed at high conversion when using **UC-5** or **SC-5** (Figures 6 and 9) suggested that these catalysts were capable of mediating intermolecular chain transfer between oligomeric macrocycles to achieve polymers of higher molecular weight. This was surprising considering that this required REMP of large, unstrained cyclic olefins. We envisioned REMP of relatively large monomers should then also equilibrate to high molecular weight polymer, despite relatively low disparity in the ring strain of each species.

To obtain appropriate monomers, we took advantage of the entropically driven ring-chain equilibria in ROMP, where unstrained macrocycles are preferentially formed below the critical monomer concentration.[20,36-40] We prepared COE macrocycles at 0.1 M, using **SC-5** as the catalyst to avoid potential linear contamination. Analysis of the product mixture via $^1$H NMR spectroscopy, GC-MS, and GPC collectively indicated that no linear contaminants or polymeric species were present. When solutions of COE macrocycles in $PhCH_3$ (olefin concentration = 0.5 M) were heated at 40 °C in the presence of **SC-5**, the reaction mixtures became more viscous indicating an increase in molecular weight. After 12 h, the PCOE was isolated in 70% yield via precipitation into acetone. GPC analysis revealed a $M_w$ of 100 kDa, consistent with the results of the molecular weight equilibration starting from high molecular weight PCOE (see above). The same final $M_w$ was obtained for $[\text{olefin/Ru}]_0$ = 500:1 and 150:1, and remained

unchanged upon isolation of polymer and re-injection of new catalyst under the same experimental conditions, suggesting that the ring sizes had reached the most thermodynamically stable state under these conditions.

**Determination of Residual Ruthenium.** As described previously, incomplete catalyst release from cyclic polymers will result in residual Ru within the polymer backbone. In addition to compromising the overall purity of the polymer products, the metal centers may decompose during subsequent workup, processing, or reactions. Unfortunately, catalyst cleavage using terminating agents such as ethyl vinyl ether, which are widely used to cleave catalyst off polymer prepared via ROMP, cannot remove the incorporated catalyst from the polymer and may also introduce linear impurity.

Therefore, the determination of the residual Ru content in the cyclic polymers obtained via REMP is crucial. Our conclusions thus far have been that catalyst release (i.e., to reform the initial cyclic catalyst) is favored for 5-carbon tethered complexes (e.g., **UC-5** and **SC-5**), and disfavored for complexes bearing longer tethers. Although solution NMR spectroscopy and kinetic data corroborate these findings, we sought a more accurate means to determine the amount of residual Ru in the cyclic polymers. Thus, we prepared samples of PCOE from various cyclic catalysts and analyzed the residual Ru content via inductively coupled plasma mass spectroscopy (ICP-MS). For comparison, linear polymer samples prepared using complex **1** were also analyzed.

Polymerizations were conducted using COE monomer (0.5 M in $CH_2Cl_2$) and $[M/Ru]_0 = 1000:1$. Upon completion, reaction mixtures were diluted to half concentration with $CH_2Cl_2$ and cooled to 0 °C causing crystallization of PCOE out of solution. The PCOE was collected and recrystallized three times from $CH_2Cl_2$ to remove most of the

unbound catalyst. To produce solutions for analysis via ICP-MS, polymer samples were digested in a mixture of concentrated $H_2SO_4$ and concentrated $HNO_3$ for 2 days at 70 °C, during which time complete dissolution of polymer was achieved. ICP-MS experiments were conducted in duplicate and a calibration curve was used to determine the amount of Ru in each sample; key data are summarized in Table 3.

The theoretical maximum Ru that could be present in the polymers at a $[M/Ru]_0$ = 1000:1 is 6,550 ppm. PCOE prepared from **UC-5, SC-5** and **UC-6** (entries 3 – 5) were found to contain similar residual Ru content of only ca 230 ppm Ru. In contrast, PCOE prepared using **SC-6** (entry 6) was found to contain 609 ppm Ru. This is consistent with previous NMR spectroscopic experiments which indicated that **SC-6** can gradually incorporate into the polymer backbone, while the incorporation of **UC-5** and **SC-5** was not observed and the incorporation of **UC-6** was only minimal at elevated temperatures. Considering that a small amount of residual Ru was detectable even when complex **1** was used and catalyst cleavage was performed at the end of ROMP (entries 1 and 2), we speculate that the consistent amounts of residual Ru from samples prepared using **UC-5**, **SC-5** and **UC-6** may reflect unbound, physically trapped metal species.

**Table 3.** Residual Ru amounts in PCOE (ppm) prepared by different catalysts after crystallization of polymer from solution[a]

| Entry | Catalyst | $M_w$ of PCOE (kDa) | [Ru] (ppm)[b] |
|---|---|---|---|
| 1 | **1**[c] | 80 | 151 ± 8 |
| 2 | **1**[d] | 80 | 137 ± 10 |
| 3 | **UC-5** | 560 | 236 ± 6 |
| 4 | **SC-5** | 500 | 237 ± 37 |
| 5 | **UC-6** | 340 | 219 ± 20 |
| 6 | **SC-6** | 380 | 609 ± 42 |

[a]Polymerization conditions: $CH_2Cl_2$, 40 °C, $[M/Ru]_0$ = 1000:1, $[M]_0$ = 0.5 M, 12 h. Excess ethyl vinyl ether was added at the end of polymerization only when **1** was used. [b]Analyzed by ICP-MS, experiments conducted in duplicate and averaged. [c]Crystallized once at 0 °C from $CH_2Cl_2$. [d]Crystallized three times at 0 °C from $CH_2Cl_2$.

**Polymer Characterization.** A significant challenge in characterization of REMP polymers is the confirmation of a ring topology. Differences between cyclic and linear analogues are typically elucidated via a combination of known solution properties of cyclic polymers, such as longer GPC retention times, smaller hydrodynamic radii, and lower intrinsic viscosities.[5-16,19,21-28] However, clear comparison of these properties requires the use of linear and cyclic polymers at exactly the same MW (i.e., linear precursor polymer and the cyclized cyclic polymer, if prepared via the end-linking strategy). Because REMP does not involve linear precursor polymers and it produces polymers with relatively broad MW distribution, linear polymers have to be prepared separately and it is difficult, if not impossible, to match the exact MW and MW distribution with the cyclic polymer. Although GPC coupled with a triple-detection system could provide this comparison by taking each slice of the polymer peak to

calculate the absolute MW of each point from light scattering, complications may occur, as discussed in the Appendix.

Therefore, we explored melt-state magic-angle spinning (MAS) NMR spectroscopy and mass spectroscopy analyses as viable methods for detecting linear polymer contaminants.

*NMR analysis.* $^{13}C$ NMR spectroscopy is one of the few methods that can provide quantitative information about polymer topology and microstructure, and has been widely used for the determination of branch content and tacticity of polyolefins.[41-45] The sensitivity of solution-state NMR spectroscopy is limited due to the low concentration of $^{13}C$ nuclei, and bulk samples typically suffer severe line broadening. Recently, optimized melt-state MAS NMR methodology has been developed to combine high spin concentrations and motional averaging of line broadening interactions that allows for quantitative analysis of minute chain units (e.g., long-chain branch junctions in polyethylene). Sensitivities for this technique are high, reaching 1 branch per 100,000 $CH_2$ groups.[42]

Herein, we extended this highly sensitive technique to compare linear (L) and cyclic (C) PCOE prepared from complex **1** and **UC-6**, respectively. GPC analysis revealed a $M_w$ of 220 kDa for the L-PCOE, corresponding to a DP of 2,000, and a $M_w$ of 114 kDa (DP = 1,040) for the C-PCOE. Notably, the lower DP of the C-PCOE in comparison with the L-CPOE should facilitate the detection of linear contaminants in the former. The polymer samples were melted in a sealed zirconia rotor under $N_2$ at 70 °C and melt-state MAS $^{13}C$ NMR spectra were recorded using a 7 mm MAS probe at 70 °C for ca. 13 h. The L-PCOE and C-PCOE were found to have similar trans/cis olefin ratios

(3.5:1 for L-PCOE and 4.2:1 for C-PCOE), calculated from the intense peaks from the polymer olefinic (δ = 132-129 ppm) and methylene (δ = 34-27 ppm) carbon resonances (Figure 10). These values were consistent with those obtained via solution-state $^{1}$H NMR spectroscopy. End groups in the L-CPOE sample manifested additional peaks in both the olefinic and alkyl regions of the spectrum. In contrast, these signals were not detectable for the C-PCOE, indicating a lack of end groups as expected for the cyclic topology. Considering the sensitivity of this technique, and the DP of the C-PCOE, the results indicate that no greater than 1 in 10 chains contain end groups. In other words, the sample obtained from **UC-6** was found to be >90% cyclic.

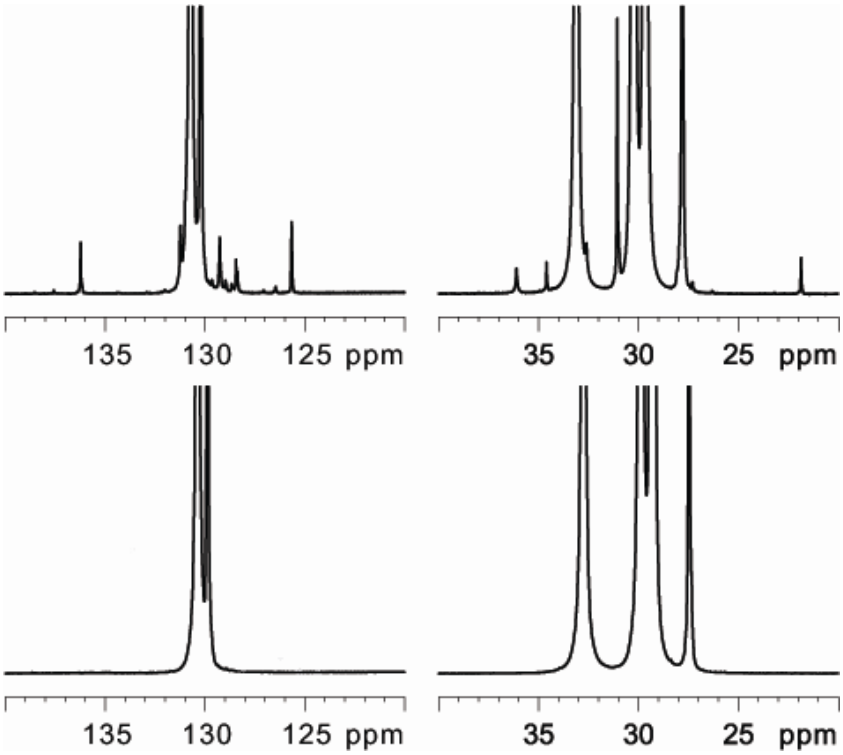


**Figure 10**. Melt-state $^{13}$C NMR spectra of linear PCOE olefinic region (top left), linear PCOE aliphatic region (top right), cyclic PCOE olefinic region (bottom left), and cyclic PCOE aliphatic region (bottom right). Linear PCOE $M_w$ = 220 kDa; Cyclic PCOE $M_w$ = 114 kDa.

*MS analysis*. We used matrix-assisted laser desorption ionization time-of-flight mass spectrometry (MALDI-TOF MS) to detect the possible end groups of polymers. Due to the extremely difficult ionization of high MW hydrocarbon polymers, poly(5-acetoxy-cyclooctene) (PCOE-OAc) was used for MALDI MS test. Both cyclic and linear PCOE-OAc was prepared under similar conditions, except for the catalyst used, with MW at ~100 kDa (Figure 11).

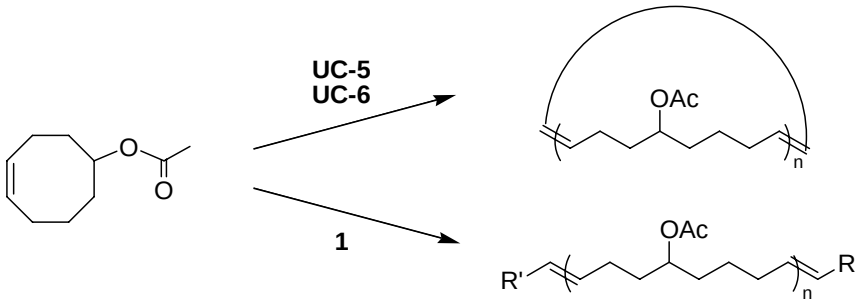


**Figure 11.** Synthesis of cyclic and linear poly(5-acetoxy-cyclooctene).

The high MW portion of PCOE-OAc was still difficult to ionize, and we obtained the spectra only for relative low MW regions (<5 kDa). MALDI-TOF mass spectrum of the cyclic PCOAc showed only the molecular ions for the sodium-complexed cyclic structure spaced in 168 Da, the molecular weight of the monomer; no other peaks with significant intensity were observed, which indicated the absence of linear structures in the range of molecular ions less than m/z 5000 (Figure 12 left). In contrast, the linear PCOE-OAc showed a group of peaks for each degree of polymerization (DP) (Figure 12 right). The assignment of end groups for these masses was difficult, but these peaks may be due to various end group decomposition during the ionization process.

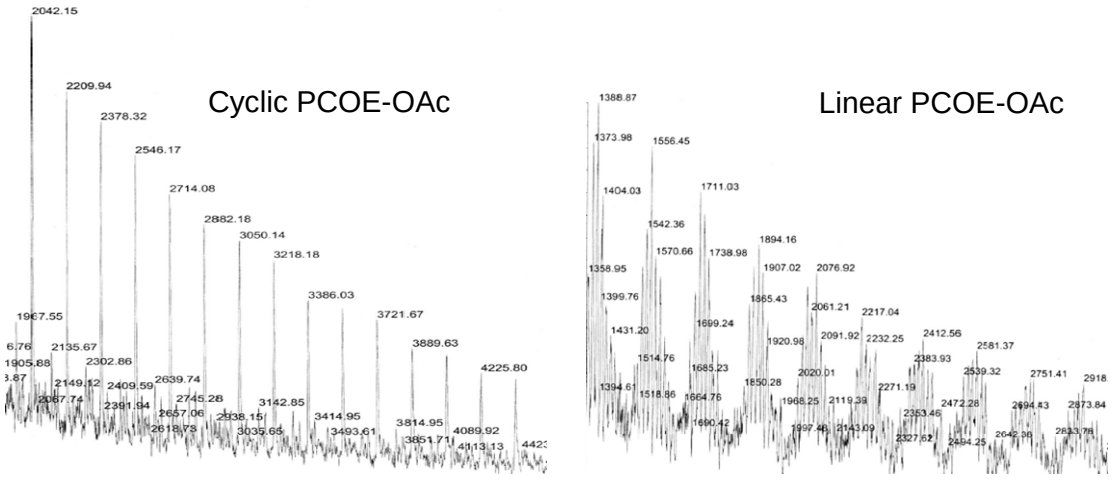


**Figure 12.** MALDI-TOF mass spectra of cyclic (left) and linear (right) poly(5-acetoxy-cyclooctene). Conditions: cyclic: [M/**UC-6**] = 200, $M_w$ = 105 kDa and linear: [M/**1**] = 500, $M_w$ = 81 kDa, at 40 °C in DCM.

## Conclusions

Ring-expansion metathesis polymerization (REMP) has been studied in detail using monomers of varied ring strain and degrees of unsaturation, in combination with cyclic Ru catalysts of varying architecture. Each key step in the proposed REMP catalytic cycle (initiation, propagation, and catalyst release or chain transfer), was probed using different catalysts. The order of initiation rates did not directly correspond to previously observed rates of polymerization, and specifically, C-5 catalysts gave faster initiation than did C-6 analogues. The catalyst tether length was found to have a significant impact on the polymerization profile: REMP using C-5 catalysts showed a step-growth like mechanism, as a result of the fast catalyst release that competed with propagation. In contrast, REMP using C-6 catalysts showed a chain-growth like mechanism, and it gave high-molecular-weight polymer before full monomer conversion due to significantly faster propagation relative to catalyst release or chain transfer. The catalyst structure controls the kinetic molecular weight of their polymer product, but after full monomer conversion the molecular weight of PCOE was found to approach an equilibrium value

that was independent of catalyst structure and initial monomer/catalyst ratios. ICP-MS analysis concluded that low levels of residual Ru were present in the cyclic polymer samples when either catalyst release was efficient (i.e., **UC-5** or **SC-5**) or catalyst incorporation was slow (i.e., **UC-6**). The cyclic nature of the polymer products was supported by high-sensitivity melt-state $^{13}C$ NMR spectroscopy and MALDI-TOF MS The reported results provide insights into the mechanism of REMP and will guide the synthesis of functional cyclic polymers and development of novel materials based on such materials.

**Experimental Section**

**Materials and instrumentation**. $CH_2Cl_2$, $PhCH_3$ and $C_6D_6$ were obtained from solvent purification columns. $CD_2Cl_2$ used for NMR scale experiments was distilled from $CaH_2$ under $N_2$ prior to use. Ru complex **1** was obtained from Materia, Inc. Cyclooctene and *cis*, *trans*, *trans*-cyclododecatriene were fractionally distilled before use. All other solvents and reagents were of reagent quality and used as obtained from commercial sources. Cyclic Ru catalysts were synthesized as described previously and stored in a glove box filled with $N_2$.[22] Solution state $^1H$ and $^{13}C$ NMR spectra were recorded using a Varian Mercury 300 or Varian Inova 500 spectrometer and were routinely run using broadband decoupling. Chemical shifts (δ) are expressed in ppm downfield from tetramethylsilane using the residual protiated solvent as an internal standard.

*Melt-state $^{13}C$ NMR spectroscopy* was recorded using a Bruker Avance 500 dedicated solid-state NMR spectrometer operating at a proton and carbon Larmor frequency of 500.13 and 125.75 MHz respectively. All measurements were undertaken with a commercial Bruker, $^{13}C$-$^1H$ optimized, high temperature, 7 mm magic-angle spinning

(MAS) probehead using zirconia rotors and rotor caps with ca. 200 mg of PCOE packed inside. $N_2$ gas was used for all pneumatics to limit thermal oxidation. All measurements were conducted at $\omega_r/2\pi$ = 3 kHz spinning speed at 70 °C sample temperature, whilst compensating for thermal MAS effects. Single pulse excitation spectra were acquired using 10 μs $^{13}C$ π/2 excitation pulses and π pulse-train heteronuclear dipolar decoupling. For both linear and cyclic PCOEs, 200 mg of polymer was used and 21,000 scans were accumulated with a 2 s recycle delay resulting in a measurement time of 13 h 35 min per sample. The spectra were normalized according to the total intensity of olefinic peaks (δ = 132-129 ppm) to compare the presence of end groups.

*Gel permeation chromatography (GPC)* was carried out in THF on two PLgel 5 μm mixed-C columns (Polymer Labs) connected in series with a DAWN EOS multi-angle laser light-scattering (MALLS) detector and an Optilab DSP differential refractometer (both from Wyatt Technology). No calibration standards were used, and d*n*/d*c* values were obtained for each injection by assuming 100% mass elution from the columns.

*Inductively coupled plasma mass spectroscopy (ICP-MS)* was conducted on a Hewlett-Packard 4500 ICP mass spectrometer (Agilent Technologies) with a CETAC ASX-500 autosampler (CETAC). PlasmaCal Ru and Rh standard solutions were used for calibration and DigitTUBEs were used for sample digestion. For sample preparation, 25 mg of polymer was accurately weighed using a microbalance and digested in a mixture of 3 mL of concentrated nitric acid and 2 mL of concentrated sulfuric acid at 70 °C for 2 days. To each digested solution was added 1 mL of a 10 ppm Rh solution, used as an internal standard for Ru. Each solution was diluted to 50 mL using DI water before analysis.

**NMR initiation kinetics.** The Ru catalyst (0.0028 mmol) was dissolved in $C_6D_6$ (0.7 mL) in an NMR tube fitted with a screw cap containing a rubber septum. The resulting solution was equilibrated in the NMR probe at 60 °C, and BVE (30 equiv relative to [Ru]) was injected into the NMR tube. Reactions were monitored by measuring the peak integration of the starting Ru-alkylidene as a function of time.

**General procedure for REMP of cyclooctene.** In a typical experiment, an oven-dried 40 mL vial with a Teflon-lined screw cap was charged with degassed COE (1.0 g, 9.1 mmol) and a stir bar. Under an argon atmosphere, 18 mL (0.5 M for the monomer) of dry, degassed $CH_2Cl_2$ or $PhCH_3$ was added via syringe. In a separate oven-dried vial, a catalyst stock solution was prepared in dry, degassed $CH_2Cl_2$ or $PhCH_3$ under an atmosphere of argon. The desired amount of catalyst was injected to the monomer solution under argon to initiate the polymerization at 40 °C. Aliquots (0.5 mL) were removed using a degassed syringe at desired time intervals and chilled with dry ice. At the end of polymerization, the solution was diluted to half concentration and was either added dropwise into 300 mL of stirred MeOH or acetone, or cooled to 0 °C in a refrigerator, and the resulting precipitate was collected by centrifugation. Isolated polymer was redissolved in THF at room temperature and reprecipitated and collected two additional times. The isolated white polymer was dried under high vacuum.

**Synthesis of macrocyclic cyclooctene oligomer using SC-5.** A 50 mL round-bottom flask filled with argon was charged with 0.3 g degassed COE and 30 mL degassed $PhCH_3$ (0.1 M). In a separate vial, an **SC-5** stock solution was prepared in degassed $PhCH_3$ under an atmosphere of argon. 2 mg **SC-5** ($[COE/\mathbf{SC\text{-}5}]_0 = 1000$) was injected into the flask. After stirring at 40 °C for 10 h, NMR showed complete conversion, and one drop of ethyl

vinyl ether was added to quench the reaction. After 1 h, all the solvent was removed under vacuum and the product passed a short silica plug eluting with hexanes to remove the catalyst. The volatiles were removed *in vacuo* to yield 0.2 g clear thick oil. $^{1}$H-NMR: $\delta$ 5.4-5.2 (m, 2H), 2.1-1.9 (m, 4H), 1.4-1.2 (m, 8H). $^{13}$C-NMR: $\delta$130.4, 129.9, 32.8, 30.0, 29.9, 29.4, 29.3, 27.5.

**References**


(1) Semlyen, J. A. *Large Ring Molecules* **1996**.

(2) Semlyen, J. A. *Cyclic Polymers, 2nd ed.* **2000**.

(3) Zimm, B. H.; Stockmayer, W. H. *J. Chem. Phys.* **1949**, *17*, 1301.

(4) Hadjichristidis, N.; Pitsikalis, M.; Pispas, S.; Iatrou, H. *Chem. Rev.* **2001**, *101*, 3747.

(5) Tezuka, Y.; Fujiyama, K. *J. Am. Chem. Soc.* **2005**, *127*, 6266.

(6) Takano, A.; Kadoi, O.; Hirahara, K.; Kawahara, S.; Isono, Y.; Suzuki, J.; Matsushita, Y. *Macromolecules* **2003**, *36*, 3045.

(7) Oike, H.; Mouri, T.; Tezuka, Y. *Macromolecules* **2001**, *34*, 6592.

(8) Lepoittevin, B.; Dourges, M. A.; Masure, M.; Hemery, P.; Baran, K.; Cramail, H. *Macromolecules* **2000**, *33*, 8218.

(9) Gan, Y.; Dong, D.; Carlotti, S.; Hogen-Esch, T. E. *J. Am. Chem. Soc.* **2000**, *122*, 2130.

(10) Yu, G.-E.; Sinnathamby, P.; Price, C.; Booth, C. *Chem. Commun.* **1996**, 31.

(11) Roovers, J.; Toporowski, P. M. *Macromolecules* **1983**, *16*, 843.

(12) Clark, P. G. G., E. N.; Chan, W. Y.; Steinmetz, W. E.; Grubbs, R. H. *J. Am. Chem. Soc.* **2010**, *132*, 3405.

(13) Qiu, X. P.; Tanaka, F.; Winnik, F. M. *Macromolecules* **2007**, *40*, 7069.

(14) Laurent, B. A.; Grayson, S. M. *J. Am. Chem. Soc.* **2006**, *128*, 4238.

(15) Schappacher, M.; Deffieux, A. *Macromolecules* **2001**, *34*, 5827.

(16) Lepoittevin, B.; Perrot, X.; Masure, M.; Hemery, P. *Macromolecules* **2001**, *34*, 425.

(17) Schappacher, M.; Deffieux, A. *Science* **2008**, *319*, 1512.

(18) Schappacher, M.; Deffieux, A. *J. Am. Chem. Soc.* **2008**, *130*, 14684.

(19) Kress, J. *J. Mol. Catal.* **1995**, *102*, 7.

(20) Reif, L.; Hocker, H. *Macromolecules* **1984**, *17*, 952.

(21) He, T.; Zheng, G. H.; Pan, C. Y. *Macromolecules* **2003**, *36*, 5960.

(22) Boydston, A. J.; Xia, Y.; Kornfield, J. A.; Gorodetskaya, I. A.; Grubbs, R. H. *J. Am. Chem. Soc.* **2008**, *130*, 12775.

(23) Jeong, W.; Hedrick, J. L.; Waymouth, R. M. *J. Am. Chem. Soc.* **2007**, *129*, 8414.

(24) Darcy A Culkin; Wonhee Jeong; Szilard Csihony; Enrique D. Gomez; Nitash P. Balsara; James L. Hedrick; Waymouth, R. M. *Angew. Chem. Int. Ed.* **2007**, *46*, 2627.

(25) Takeuchi, D.; Inoue, A.; Osakada, K.; Kobayashi, M.; Yamaguchi, K. *Organometallics* **2006**, *25*, 4062.

(26) Li, H.; Debuigne, A.; Jerome, R.; Lecomte, P. *Angew. Chem. Int. Ed.* **2006**, *45*, 2264.

(27) Kudo, H.; Makino, S.; Kameyama, A.; Nishikubo, T. *Macromolecules* **2005**, *38*, 5964.

(28) Kricheldorf, H. R. *J. Polym. Sci. Part A: Polym. Chem.* **2004**, *42*, 4723.

(29) Bielawski, C. W.; Benitez, D.; Grubbs, R. H. *J. Am. Chem. Soc.* **2003**, *125*, 8424.

(30) Bielawski, C. W.; Benitez, D.; Grubbs, R. H. *Science* **2002**, *297*, 2041.

(31) Ulman, M.; Grubbs, R. H. *Organometallics* **1998**, *17*, 2484.

(32) Bielawski, C. W.; Grubbs, R. H. *Angew. Chem. Int. Ed.* **2000**, *39*, 2903.

(33) Sanford, M. S.; Love, J. A.; Grubbs, R. H. *J. Am. Chem. Soc.* **2001**, *123*, 6543.

(34) Love, J. A.; Sanford, M. S.; Day, M. W.; Grubbs, R. H. *J. Am. Chem. Soc.* **2003**, *125*, 10103.

(35) Ritter, T. H., A.; Wenzel, A. G.; Funk, T. W.; Grubbs, R. H. *Organometallics* **2006**, *25*, 5740.

(36) Hocker, H.; Reimann, W.; Riebel, K.; Szentivanyi, Z. *Makromol. Chem.* **1976**, *177*, 1707.

(37) Chen, Z.-R.; Claverie, J. P.; Grubbs, R. H.; Kornfield, J. A. *Macromolecules* **1995**, *28*, 2147.

(38) Marmo, J. C.; Wagener, K. B. *Macromolecules* **1995**, *28*, 2602.

(39) Hodge, P.; Kamau, S. D. *Angew. Chem. Int. Ed.* **2003**, *42*, 2412.

(40) Kamau, S. D.; Hodge, P.; Hall, A. J.; Dad, S.; Ben-Haida, A. *Polymer* **2007**, *48*, 6808.

(41) Min, E. Y. J.; Byers, J. A.; Bercaw, J. E. *Organometallics* **2008**, *27*, 2179.

(42) Klimke, K.; Parkinson, M.; Piel, C.; Kaminsky, W.; Spiess, H. W.; Wilhelm, M. *Macromol. Chem. Phys.* **2006**, *207*, 382.

(43) Byers, J. A.; Bercaw, J. E. *Proc. Natl. Acad. Sci. USA* **2006**, *103*, 15303.

(44) Yoder, J. C.; Bercaw, J. E. *J. Am. Chem. Soc.* **2002**, *124*, 2548.

(45) Wood-Adams, P. M.; Dealy, J. M.; deGroot, A. W.; Redwine, O. D. *Macromolecules* **2000**, *33*, 7489.